PAPER

Check for updates

Temperature-induced diurnal redox potential in soil†

Kristof Dorau, [ID] *[a] Bianca Bohn,[b] Lutz Weihermüller [ID][c] and Tim Mansfeldt [ID][a]

With the capabilities to measure redox potentials (E_H) at a high temporal resolution, scientists have observed diurnal E_H that occur in a distinct periodicity in soils and sediments. These patterns have been disregarded for a long time because minor fluctuations of the E_H in the tens of mV range are difficult to interpret. Various explanations have been proposed for the origin of diel E_H but a cohesive assessment of the temperature-dependency for field- and laboratory-based investigations is missing at present. In this study, we investigated spatiotemporal diel E_H of previous long-term (up to 10 years) field- and lab-based monitoring data collected at high-temporal (every hour) and spatial (up to 6 depths) resolution. In addition, we set up a redox experiment where we manipulated the soil temperature (ST) by diel temperature cycles to assess the E_H response. Diel fluctuations were absent for laboratory experiments with ΔE_H of a few mV (daily $E_{H\text{-max}}$ − daily $E_{H\text{-min}}$), but we found pronounced fluctuations up to ∼100 mV for field investigations. The spatiotemporal pattern in E_H fluctuations was amplified in the topsoil during the summer months concomitant with ST. We showed for the first time that changes in ST during an incubation experiment altered the E_H by −3.3 mV °C^{-1} and inferred that the diel E_H were driven by the thermal conditions of the soil itself. This is particularly important when E_H is measured close to the soil surface and underlines that minor fluctuations of the E_H with a recurring periodicity should be carefully checked for its dependency with the soil and reference electrode temperature. Redox measurements should not be considered a routine determination and cautious handling of E_H data by physical sound corrections is urgently needed in order to link ΔE_H to daily biogeochemical cycling in soils.

Environmental significance

The coherent interpretation of redox potential (E_H) measurements in soils and sediments is difficult from a theoretical and practical perspective. Spatiotemporal patterns of E_H are controlled by intrinsic soil properties as well as external factors. In our study, we highlighted that the thermal conditions of the soil itself largely explain the diel E_H by −3.3 mV °C^{-1}, a finding that has been overlooked so far. When working with automatic redox measurements on a high temporal scale, a diel E_H should be verified for its temperature dependency and not be misinterpreted, *e.g.*, as exclusively microbial-related features that occur in soils.

1 Introduction

Automated and continuous data logging of redox potential (E_H) in soils is beneficial to delineate their redox status, which is crucial to assess the mobility of trace metals,[1] nutrients,[2] greenhouse gas emission,[3] biotransformation of organic pollutants,[4] isotopic fractionation processes,[5] and soil genesis.[6]

[a]University of Cologne, Faculty of Mathematics and Natural Sciences, Department of Geosciences, Institute of Geography, Albertus-Magnus-Platz, D-50923 Köln, Germany. E-mail: k.dorau@uni-koeln.de

[b]University of Cologne, Faculty of Mathematics and Natural Sciences, Department Didactics of Mathematics and Natural Sciences, Institute of Physics Education, Albertus-Magnus-Platz, D-50923 Köln, Germany

[c]Forschungszentrum Jülich GmbH, Agrosphere Institute IBG-3, Leo-Brandt-Str., D-52426 Jülich, Germany

† Electronic supplementary information (ESI) available. See DOI: 10.1039/d1em00254f

Measurements, *e.g.*, on an hourly basis, became technically feasible several decades earlier,[8,9] which paved the way to assess the dynamic nature of the E_H. Since then, numerous authors have reported that diurnal E_H have occurred in soils with daily cycles up to 200 mV.[10–12] Even at 2 and 8 m depths of a sandy aquifer pronounced fluctuations up to 50 mV in E_H were found.[13] While some studies did not pay any attention to this phenomenon,[12,14] others gave various explanations. These included, for instance, the temperature in general as part of the Nernst equation,[10] temperature-dependent O_2 solubility,[13] changes in light intensity that impacted photosynthetic activity in plants,[11] and recently, a universal periodicity in atmospheric electricity that affects microbial processes in soil and thus redox conditions with a diel E_H.[15] In addition, it was recently shown that barometric-pumping alters the gas transport in soils and this might be a factor for diel E_H.[16] However, besides these plausible processes it is well known that temperature affects the

standard potential (E^0) of the reference electrode but this technical related issue has not been systematically cross validated with data from the field. A linkage between spatiotemporal trends in diel E_H and how this is related to the soil temperature (ST) is missing up to now.

Diel E_H cycles were omnipresent during our own previous monitoring campaigns, but we did not pay close attention to these patterns, nor did we speculate about their origin.[1,6,17] We did this in line with the current belief that variations in electrochemical force up to 50 mV have little meaning and cannot be interpreted.[18] To appropriately measure E_H, the basic equipment includes (i) redox electrodes, (ii) a reference electrode, (iii) a salt bridge, and (iv) portable voltmeters or data loggers.[7] There is an undoubted value to employ E_H measurements to obtain a mechanistic understanding of temporarily water-saturated soil environments.[6,19–21] However, a quantitative interpretation of the E_H is only valid under chemical equilibrium conditions. This thermodynamic prerequisite is in most cases not met, since the electron pool in soils changes continuously due to soil organic matter (e^- donor) turnover.[7] Furthermore, the limitation of electroactive redox couples in soil solution with concentrations $<10^{-5}$ M, e.g., Fe(III) and Fe(II), featuring rapid and reversible electron transfer reactions[22,23] allows only for the determination of redox classes rather than absolute values. Even though E_H is considered a master variable along with pH and has proven to be an attractive measure the manifold limitations of this concept tend to be neglected.[24]

To investigate the spatiotemporal diel E_H more into detail, we looked at our own previous field data where E_H was measured to delineate reducing conditions, but this time, we focused particularly on diurnal variations that were analyzed by a time-series analysis. The data comprises three long-term field data sets that extend from 18 months to 10 years and multiple laboratory-based experiments that lasted up to one year. Both generic settings featured in total 50 individual electrodes and a raw data set of 7×10^6 individual E_H measurements to derive trends in diel E_H.

2 Materials and methods

2.1 Study sites

We used data from previous field and laboratory experiments and focused on diurnal E_H variations. The study sites were in Germany: two in North Rhine-Westphalia (Lavesum 51°48′59″ N,

7°12′59″ E, 41 m asl; Kottenforst 50°40′18″ N, 7°02′48″ E, 168 m asl) and one in Schleswig-Holstein (Speicherkoog 54°8′1″ N, 8°58′28″ E, 0.5 m asl). The sites differed in land use (Table 1). It is a common feature that the soils were temporally affected by reducing conditions either due to groundwater (the Gleysols) or perched water (the Planosol). In addition, the soils featured a broad range of relevant properties from carbonaceous-rich soil with neutral soil reaction to low-pH environments (Table 2). For a detailed site description the reader is referred to Mansfeldt and Overesch,[1] Dorau and Mansfeldt,[17] and Dorau et al.[6]

2.2 Data collection in the field

Each monitoring campaign comprised a variable period with the longest duration for Speicherkoog, followed by Kottenforst, and finally by Lavesum (Table 1). The measurement interval was on an hourly basis, and the data were stored in a data logger (enviLog Maxi, ecoTech, Bonn, Germany). We employed permanently installed platinum (Pt) electrodes for each site, and a silver–silver chloride (Ag–AgCl; 3 M KCl internal electrolyte) electrode served as the reference. The reference electrode (ecoTech, Bonn, Germany) was pushed in a salt bridge,[25] which was a perforated PVC tube filled with 3 M KCl and stabilized by agar, to slow down the loss of KCl solution through the diaphragm. The Pt electrodes (ecoTech, Bonn, Germany) were placed in stellar configuration around the reference electrode and the measured voltage was corrected by adding +207 mV, i.e., the deviation against the standard hydrogen electrode at 25 °C. The E_H readings were not adjusted to pH 7 because the use of the Nernst factor for soils is questionable[26] but in any case, the pH of the respective sample should be reported (Table S1†). At each study site, the individual Pt electrodes were physically separated from the reference electrode, and the galvanic circuit was connected by a relay only for the measurement itself. A multiplexer was programmed to measure each channel with 12.5 ms, and a subsequent stabilization time of 200 ms before the next channel was measured. To obtain a stable and precise reading, all data loggers featured a high impedance of >1 TΩ (enviLog module, ecoTech, Bonn, Germany) with an AD converter of 16 bit resolution and a measurement range from −1250 to +1250 mV. Per soil depth, each three Pt electrodes attached to 5 m shielded Cu cables (distance from the Pt tip to the data logger) were installed at variable depths (Table 1). An important feature was that at all sites the redox electrodes had

Table 1 Relevant information about the study sites in Germany where redox potential monitoring was conducted

Study site	Land use	Soil type[a]	Monitoring period	Measurement depths (cm)	Parameters measured
Lavesum	Extensively used grassland	Haplic gleysol (petrogleyic)	July 2006 to February 2008	10/20/30/50/80/120	ST[b]
Speicherkoog	Non-cultivated grassland	Calcaric gleysol (eutric)	April 2010 to September 2020; ongoing	10/20/30/60/100/150	ST, AT[c]
Kottenforst	Forest	Epidystric albic planosol (ferric)	April 2014 to September 2020; ongoing	25/65/90/120	ST

[a] According to WRB.[36] [b] Soil temperature. [c] Air temperature.

This journal is © The Royal Society of Chemistry 2021

Environ. Sci.: Processes Impacts, 2021, **23**, 1782–1790 | **1783**

the same design, *i.e.*, a Pt wire of 1 mm in diameter and 5 mm in length protruded into the soil. This ensured that a uniform electrode surface area of ∼15.7 mm^2 was in contact with the soil matrix. The Pt wire was welded on a copper (Cu) wire that was connected to a standard Cu cable. Soil temperature was simultaneously measured at all redox electrode depths with Tensiomark® and pF Meter (ecoTech, Bonn, Germany) at Kottenforst and Speicherkoog and temperature sensors (Pt 100) at Lavesum. The air temperature was exclusively measured at Speicherkoog using a weather transmitter (WXT520, Vaisala, Helsinki, Finland).

2.3 Data collection in the laboratory

The redox electrodes employed for the lab experiments were identical in construction with the ones employed for the field investigation, which was also true for the reference electrode and the data logger. Thereby, the installation was carried out either in (i) homogenized and air-dried soil sieved <2 mm or (ii) undisturbed samples taken by steel cylinder (250 cm^3) in which the redox electrodes were installed. The room for the incubation experiments was air-conditioned and kept constantly at 25 ± 2 °C.

2.4 Incubation experiment with manipulated temperature

To check for the impact of temperature, we excavated an undisturbed soil monolith (20 × 20 × 5 cm; l × h × w) by an acryl glass housing from the Speicherkoog study site (labeled as "Lab E" in Table S1, Fig. S1†) and installed redox electrodes at depths of 2.5, 7.5, 12.5, and 17.5 cm. The test assembly was incubated in a climate chamber (KB400, Binder, Tuttlingen, Germany) and the temperature was (i) adjusted at a constant value of 25 °C for two months, (ii) raised to 35 °C and then lowered to 15 °C in 5 °C increments for every three days, and (iii) manipulated to fluctuate daily between 35 and 15 °C. The experiment at constant temperature (25 °C) was at first performed under reducing conditions by adjusting the water table in the box to 10 cm below soil depth followed by re-aeration of the sample *via* removal of the soil water due to free drainage. The temperature manipulation between 35 and 15 °C reflects a typical daily air temperature range found in mid-latitude regions during cloudless conditions. For this particular experiment, the Ag–AgCl reference electrode remained for the first half of the experiment inside the soil and, thus, was also prone to changes in temperature. For the second half, we detached the electrode from the soil and connected it *via* an electrolyte bridge from outside the climate chamber. Thus, only the Pt electrodes and the soil were affected by temperature changes. The electrolyte bridge was a silicone tube (1 cm Ø) filled with 3 M KCl and stabilized by agar.

2.5 Statistical analysis

Since we employed only quasi-stationary E_H conditions where the focus is on the diurnal E_H variability with a recurring periodicity, we removed periods with a strong E_H increase or decrease, *e.g.*, due to the position of the variable water table. These transitions across multiple redox classes are typical in waterlogged horizons with changes up to 540 mV within 24 hours[17] but would potentially bias our analysis. Neglecting these transitions curtailed the data but by doing so we reduce overfitting and focus on diel E_H with the underlying mechanistic relationships (Fig. S2†). In addition, we deleted data from measurements when the E_H exceeded 50 mV within one hour and classified this data as unsuitable (not available; NA) for our calculations. All analysis including data manipulation, calculation, and visualization were carried out in R.[27] The most important steps featured (i) aggregation of the hourly data to calculate the range between daily min and daily max denoted with delta (Δ) in the following, (ii) summarization of the data to allocate the monthly mean throughout the time-series, and (iii) summarization of the data for the distinct hour of the day. All steps were done for the individual electrodes (in triplicate per depth) and joined afterward, when needed, to obtain the depth-specific mean and the standard error of the mean.

2.6 Soil properties

The most important soil properties for both the field and the lab were determined at oven-dried and sieved (<2 mm) samples as follows: pH was measured using a glass electrode in a 0.01 M L^{-1} CaCl$_2$ solution mixed 5 : 1 with soil (vol/vol);[28]

Table 2 Overview of studies that observed diel E_H with the employed technical equipment

Study	Authors	Setting	Diel E_H	Distance between Pt and Ag–AgCl electrode	Reference electrode
Lab	37	Mollic gleysol	NO (soil columns)	A few cm	3 M Ag–AgCl
	14	Silt-loam argixeroll	YES (PVC rings)	A few cm	3 M Ag–AgCl
Field	38	Saltmarsh sediments	YES (4)	Combination electrode	n. m.
	39	Tidal wetland	YES (20/50)	∼50 cm	Calomel
	12	Humic gleysol	YES (5/20/30)	∼30 cm	4 M Ag–AgCl
	10	Saltmarsh	YES (1/2/4/5/9/10)	A few cm	Calomel
	40	Reed bed	YES (20)	From 1 to 15 m	Ag–AgCl
	13	Peat and sandy aquifer	YES (19/25/35/109/119/200/800)	From a few cm to 8 m	Ag–AgCl
	17	Calcaric gleysol	YES (10/20/30/60/100/150)	∼50 cm	3 M Ag–AgCl
	41	Tidal soil	YES (15/25/50/75)	n. m.^{a}	Ag–AgCl
	15	Synthetic substrate	YES (50/100)	n. m.	Calomel

^{a} Not mentioned.

1784 | *Environ. Sci.: Processes Impacts*, 2021, **23**, 1782–1790

This journal is © The Royal Society of Chemistry 2021

organic carbon (OC) using a CNS analyzer (Vario EL cube, Elementar, Hanau, Germany);[29] the particle-size-distribution after pre-treatment with H_2O_2 and HCl by the sieve and settling method.[30]

3 Results and discussion

3.1 Prominent temperature effects on E_H measurements

The temperature has a manifold impact on the E_H measurement because it (i) is an inherent property of the Nernst equation, (ii) changes the electrical properties of the cabling, and (iii) alters the electrode potential of the reference electrode. First, if we consider a common redox reaction with $Fe^{3+} + e^- \rightleftharpoons Fe^{2+}$, having a standard potential (E^0) of 770 mV and assuming equilibrium conditions, temperature modifies the measured potential by, however, only 0.086 mV °C^{-1} (Fig. 1A). Second, the cabling to measure redox consists of a conducting cable (e.g., a Cu cable with 5 m length and 1 mm Ø; as is employed for the field experiments), and along with an increase in temperature, the electric resistance increases by 0.442 mΩ °C^{-1} (Fig. 1B). Brownian motion is responsible for this behavior because as more atoms and molecules bounce around, e.g., within a Cu cable, the harder it is for electrons to flow. However, if we consider a typical exchange current of 1 μA at the Pt surface, these marginal changes in R along with the associated little currents can only explain <0.001 mV °C^{-1} and, thus, resistance of the Cu cable is not a factor. Third, the Ag–AgCl (3 M KCl) reference electrode has a fixed E^0 of 207 mV at 25 °C, but temperature modifies the measured E_H relative to the reference electrode by −0.71 mV °C^{-1} (Fig. 1C). Temperature fluctuations of 20 °C would explain a variation of 14 mV from the reference electrode, but this can barely explain fluctuations in ΔE_H up to

50 mV and even larger.[10,15,17] Finally, the temperature of the measured medium is also of importance, as exemplified with ZoBell's solution. This test solution is classically employed to check for the proper functioning of the redox electrodes and shows an inherent strong temperature dependency due to entropy, enthalpy, and heating capacity with −2.40 mV °C^{-1} (Fig. 1D).[31] However, up to now the temperature of the measured medium, i.e., the soil, has not been included in the E_H measurement protocol.

3.2 Temperature effects in the laboratory

To verify the key role of temperature on the E_H measurement, we set up an incubation experiment in the laboratory (Fig. S1†). Under constant temperature of 25 °C (Fig. 2A), we did not observe diel E_H under reducing conditions when the water table was adjusted at 10 cm below soil depth (in 7.5, 12.5, and 17.5 cm), or under oxidizing conditions subsequent when the sample was aerated from 27 July onwards (Fig. 2B). All electrodes reached quasi-stationary E_H conditions on 22 August, and from this moment on, we adjusted the temperature in a stepwise manner (Fig. 2A). Interestingly, the E_H reacted instantaneously after each temperature change (Fig. 2B), and under quasi-stationary conditions, a significant negative correlation between E_H and temperature existed ($r = -0.995$, $p < 0.001$; Fig. 2C). As soon as we generated daily temperature fluctuations, we produced a periodicity in E_H in all depths with a clear cause-effect relationship (Fig. 2B). Thus, we argue that temperature is involved in the development of daily E_H cycles with our empirical data highlighting a slope of −3.3 mV °C^{-1}, if we correct the measured E_H for the temperature-dependency of the reference electrode (Fig. 2C). To the best of our knowledge,

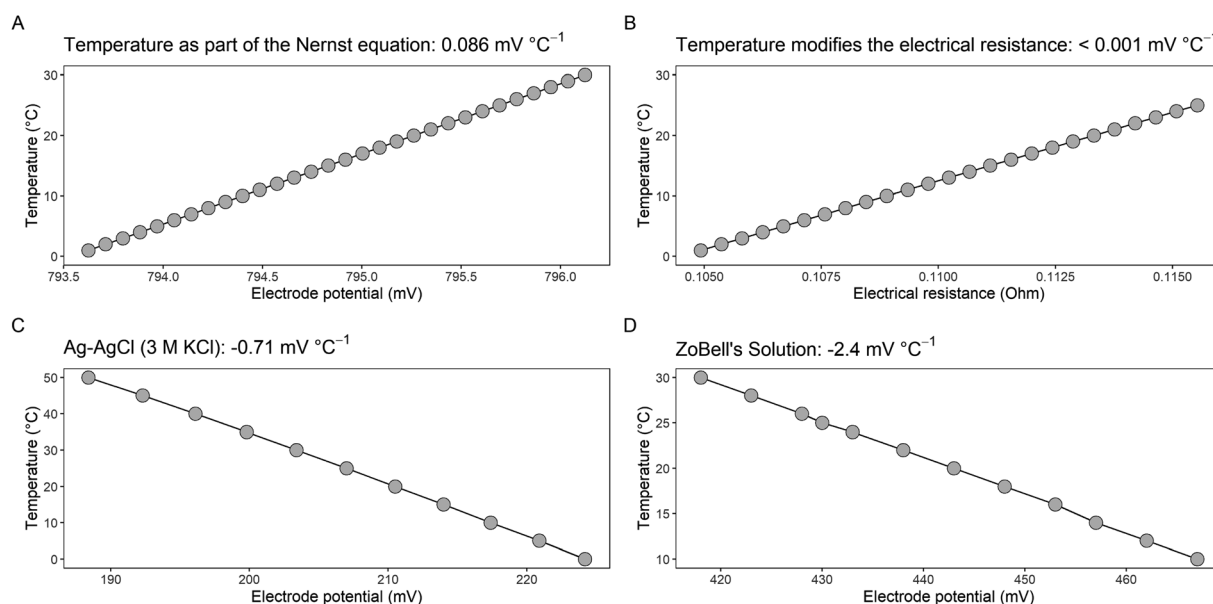**Fig. 1** Temperature-dependent impact with respect to the Nernst equation by consideration of the reaction $Fe^{3+} + e^- \rightleftharpoons Fe^{2+}$ (E^0 770 mV) (A), changes of electrical resistance (Ω) for a copper cable (5 m length and 1 mm Ø) (B), and alterations on electrode potential from an Ag–AgCl reference electrode (3 M KCl L^{-1} internal electrolyte; C). The temperature of the measured medium is also of importance and shown for ZoBell's solution (D). Data for the calculations were taken from Strawn et al. (A),[42] Hering et al. (B),[43] Galster (C),[44] and Nordstrom (D).[31]

This journal is © The Royal Society of Chemistry 2021

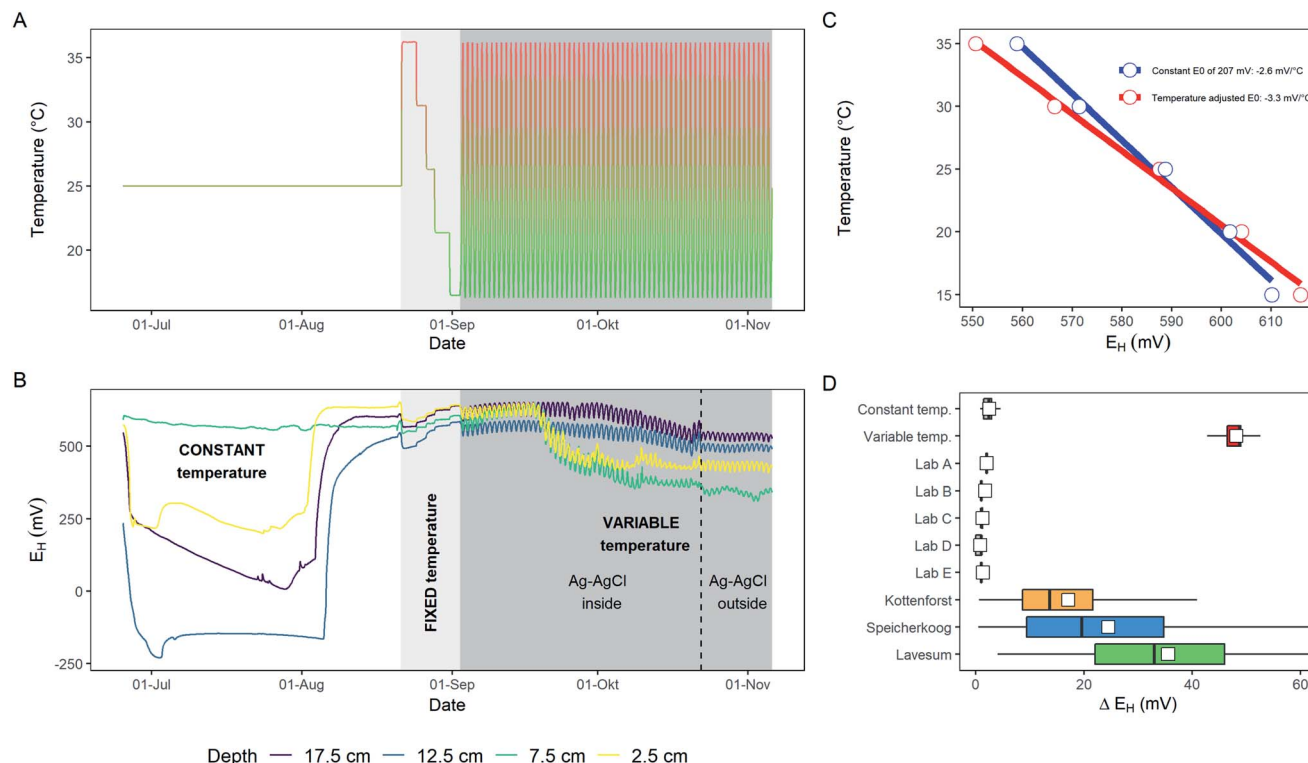Environ. Sci.: Processes Impacts, 2021, **23**, 1782–1790 | **1785**

Fig. 2 Development of temperature (A) and redox potential in four depths (E_H; B) for a soil monolith incubated within a climate chamber. The climate chamber was programmed to run under three different conditions: (i) constant temperature, (ii) fixed temperature, and (iii) variable daily temperature regime. We used the following equation and corrected the measured voltage by adding the temperature-dependent deviation against the standard hydrogen electrode: $E_H = (-0.714 \times \text{temperature}) + 225$ (see Fig. 1C). The regression lines in (C) were derived from the fixed temperature conditions and account for the applied correction (red) and assuming a constant temperature of 25 °C by adding +207 mV to adjust the measured voltage (blue line). Under variable temperature regime, the experiment was conducted with the reference electrode (Ag−AgCl; 3 M KCl internal electrolyte) being inside the climate chamber and put outside on 22 October outside the climate chamber. The electrical circuit with the soil was closed via an electrolyte bridge. Panel (D) shows the mean ΔE_H (calculated as the difference between daily $E_{H\text{-max}} - E_{H\text{-min}}$ value) for the redox incubation experiment under constant and variable temperature, for previous lab experiments (Lab A to E), and for field experiments (Kottenforst, Speicherkoog, Lavesum) among all electrodes and different depths.

the only study performed in the laboratory that exhibited a diel E_H was by Wanzek et al.,[14] and just as in our experiment, their setup mimicked ambient conditions outside the greenhouse, i.e., with cyclic changes in temperature (Table 2). However, in most cases experiments in the laboratory are performed under constant room temperature. Indeed, all our previous lab experiments revealed $\Delta E_H < 3$ mV, which was true for homogenized soil (Lab A to Lab C) as well as for undisturbed samples taken from the field (Lab D to Lab E; Fig. 2D). Contrary to the experiments performed with a constant ST, our field data and the data from this study under variable temperature demonstrated considerable ΔE_H with on average 18 mV for study site Kottenforst and up to 50 mV within this study under variable temperature (Fig. 2D).

3.3 Temperature effects in the field

As previously mentioned, diel E_H with a recurring periodicity were omnipresent during our field campaigns among all depths and electrodes for all sites (Fig. S3D–F†). The average ΔE_H decreased in the order Lavesum > Speicherkoog > Kottenforst (Fig. 2D). Thereby, diel E_H occurred under strongly reducing conditions for some electrodes at Speicherkoog and Lavesum

(Fig. S3A and B†) but also under oxidizing conditions with $E_H >$ 300 mV predominant for Kottenforst (Fig. S3C†). Temperature fluctuations are most pronounced at the soil surface and this is coherent with a decrease in ΔE_H for Lavesum and Speicherkoog (Fig. S4†). The absence of this pattern for Kottenforst is plausible, because the forested site is shaded by the canopy and the upper most depth in 25 cm generally exhibits only marginal changes in ST.

For the monthly development in ΔE_H, there was an annual pattern evident for the 10 cm soil depth that peaked during the summer months with values up to 50 mV in conjunction with ΔST (Fig. 3A and B). If these patterns are broken down on a daily basis, the E_H was lowest when the ST was highest (Fig. 3C and D; $r = -0.99$, $p < 0.001$), in accordance with the negative correlation of the independent laboratory-based study with -3.3 mV °C^{-1} (Fig. 2C). ΔE_H in 150 cm soil depth was considerably lower with annual values between 5 to 10 mV, since there are neither annual nor daily variations in ΔST. Thus, no significant correlation existed with ST in this depth but the daily curves between E_H and air temperature matched perfectly ($r = -0.94$, $p < 0.001$; Fig. S5B†). We assume two different mechanisms being important for this finding, which are (i) changes of the reference
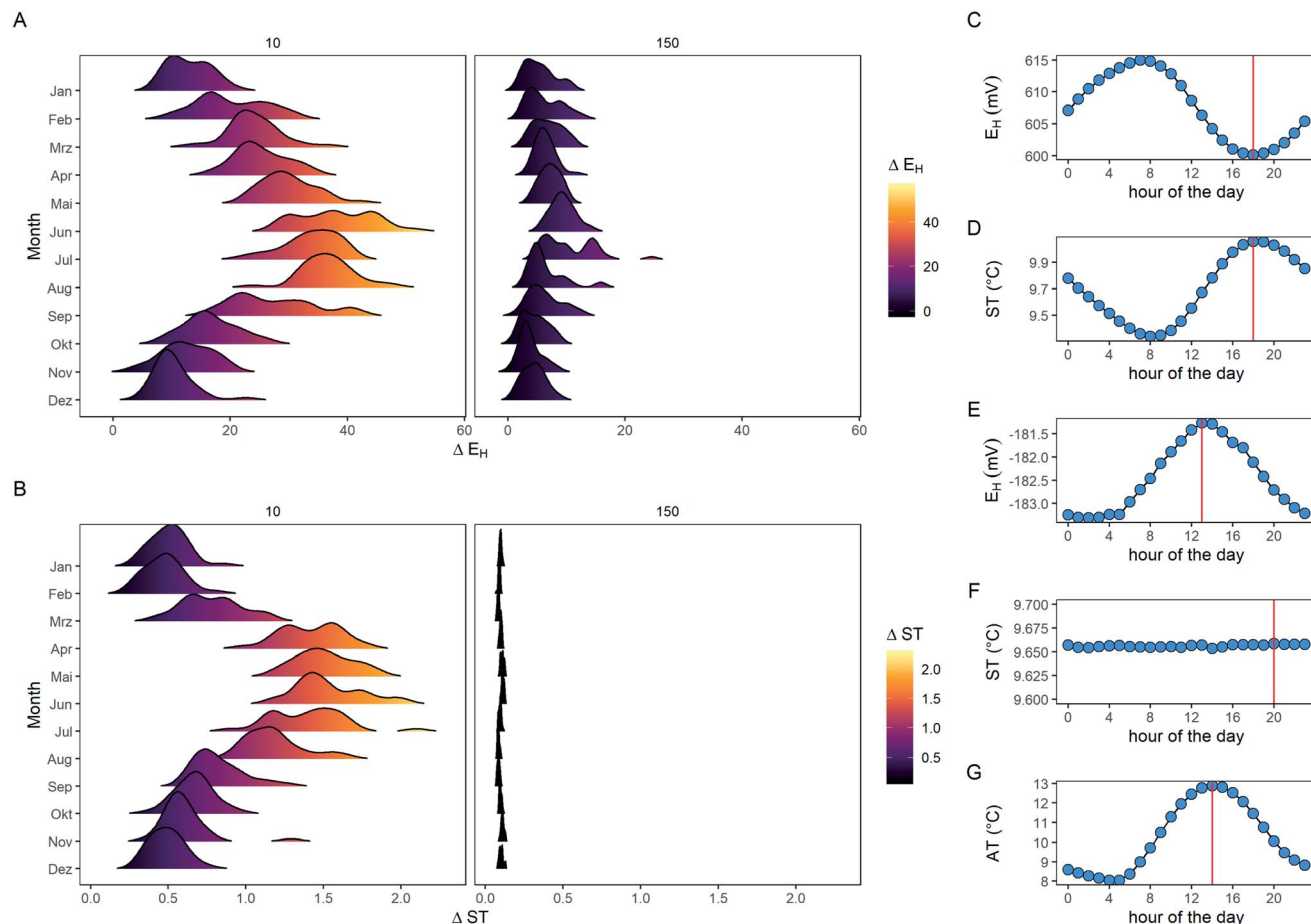
Fig. 3 Data density distribution visualized by ridgeline plots of delta redox potential (ΔE_H; A) and soil temperature (ΔST; B) in 10 and 150 cm soil depth across the individual months. In addition, information about the daily pattern with mean E_H and ST for a single electrode in 10 cm (C and D) and 150 cm depth (E and F), as well as air temperature (AT; G) is plotted for each hour of the day. The red lines (C to G) indicate the maximum value for each variable and the spatiotemporal pattern are averaged for a 10 year study exclusively from site Speicherkoog.

electrode temperature and (ii) the thermal properties of the soil. The E_H measurement procedure in our study – and in most of the other field studies (Table 2) – features a two-probe system with a separated reference and redox electrode. This has practical advantages compared with a combination electrode in terms of maintenance and costs. However, since the reference electrode is positioned at the soil surface (Fig. S6†), its standard electrode potential is more affected by changes in AT than ST. Thus, E_H measured in subsoils will only be affected by changes of the reference electrode temperature while E_H measured in the topsoil is in addition affected by the thermal properties of the soil itself. The latter process contributes largely to the magnitude of diel E_H. Overall, a temperature correction of the E_H is particularly desirable if measurements are conducted within surface horizons where daily amplitudes in ST are expected, *e.g.*, in the summer time.

3.4 E_H correction for temperature fluctuations

Strong indication that fluctuations in ST has to be taken into account for correcting periodicity in measured E_H, even if the reference electrode is placed in an environment with constant

temperature, is provided in Fig. 2B, where E_H is measured in the climatic chamber and the reference electrode is located outside the climate chamber. For the temperature correction of E_H a detrending approach was applied, as commonly done to correct, *e.g.*, soil CO_2 flux measurements performed over the course of a day with varying temperature[32] according to eqn (1):

$$E_{H\ corrected} = E_H + (\text{MST} - \text{ST}) \times m \tag{1}$$

where E_H is the measured redox potential (mV) measured at a specific time, ST is the soil temperature (°C) at the time E_H was measured, MST is the mean soil temperature (°C) over the entire measurement period, and m is the slope from the regression equation between E_H and ST over the course of the measurement period. In our case m was calculated to be −7.58 in the example of Fig. 4A. Applying this correction to the measured E_H resulted in a decreased ΔE_H from 34 ± 16 mV for the raw data towards 16 ± 9 mV for the corrected E_H (Fig. 4B). Even if this straight forward approach already improved the ΔE_H substantially, more sophisticated correction approaches are desired. For instance, the data in Fig. 4A clusters into two groups due to (i) a general soil warming/cooling trend from the 22nd of June
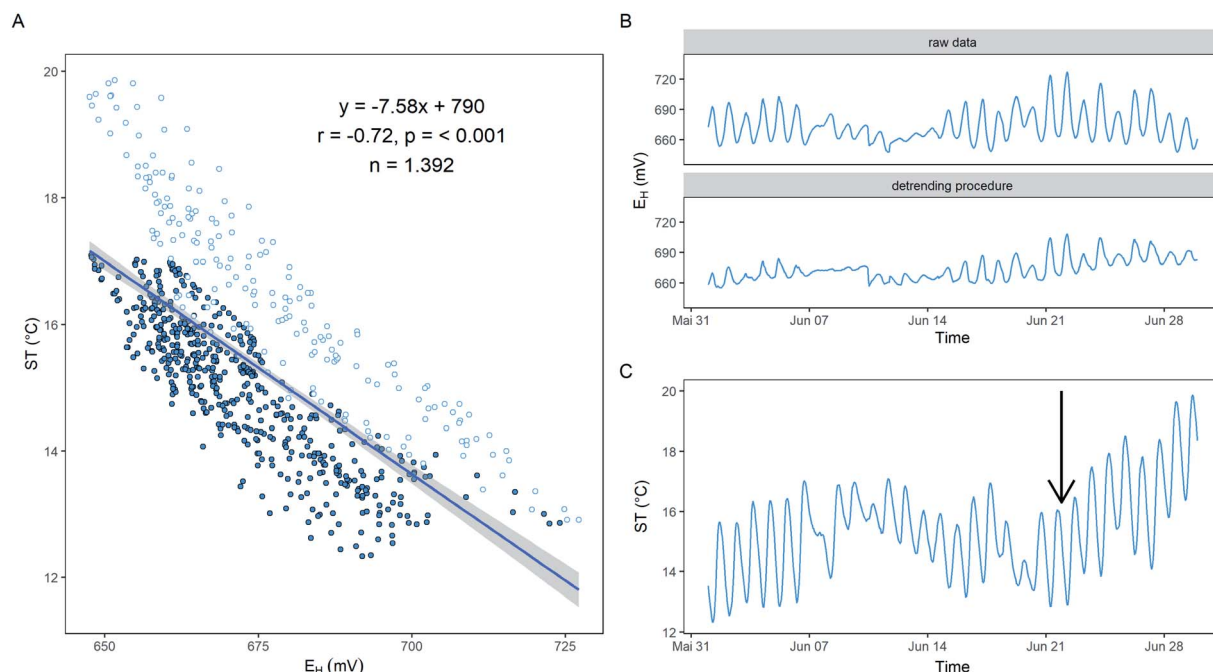
Fig. 4 Linear regression between soil temperature (ST) and redox potential (E_H) (A) for the period under investigation (B and C). Raw E_H data (upper panel B) was corrected according to Eq. [1] and are depicted in the lower panel (B). The data accounts for a single electrode and for a one-month period at site Speicherkoog in 10 cm depth. Please note, the data clusters from the 22nd of June onwards (arrow in C) that results into a branch driven by warming/cooling of the soil (hollow blue dots; A) and one branch that reflects a diel E_H driven by day–night cycles (solid blue dots; A).

onwards, and (ii) cyclical alterations due to day–night cycles. More adaptive mathematical algorithms should cope with these constraints but the ultimate goal would be a physical based correction method that integrates geochemical data such as PHREEQC[33] with heat-, water-, and gas-transport to explain diel E_H in soil. The HP1 software[34] offers such capabilities but the main challenge remains to feed these physical trained models with data collected as close as possible in vicinity to the Pt surface of the redox electrode. Recently, Maisch *et al.*[35] collected by noninvasive imaging techniques Fe(II), Fe(III), O_2, and pH gradients at high temporal (hourly) and spatial (~mm) scale within specialized rhizotrons filled with an artificial substrate. This points to the right direction to further investigate highly variable E_H patterns in soil by knowledge of the environmental surrounding. Whereas the correction of E_H has no impact on long-term trends it should be considered as a first step to reduce technical noise and artefacts being present in E_H data.

4 Conclusions

Diel variations in E_H were omnipresent when monitoring was performed in the field and showed an (i) annual, (ii) daily, and (iii) soil depth-dependent pattern. Enhanced diurnal fluctuations in soil temperature were linked to diel changes in E_H and were amplified during the summertime. In addition to the theoretical restrictions that are accompanied by E_H measurements using a Pt electrode, the temperature of the soil itself must be integrated simultaneously with the well-known temperature-dependence of the reference electrode. The temperature of the soil itself changes its thermochemical behavior analog to ZoBell's solution[31] and this should be carefully considered to partition and discriminate between physical and biological influences on the E_H measurement. Therefore, physical sound corrections should be further pursued in the future to differentiate between technical related noise and microbial-driven signals on redox measurements.

Conflicts of interest

There are no conflicts to declare.

Acknowledgements

References

1 T. Mansfeldt and M. Overesch, Arsenic mobility and speciation in a Gleysol with petrogleyic properties: a field and laboratory approach, *J. Environ. Qual.*, 2013, **42**, 1130–1141, DOI: 10.2134/jeq2012.0225.

1788 | *Environ. Sci.: Processes Impacts*, 2021, **23**, 1782–1790

This journal is © The Royal Society of Chemistry 2021

2 T. Peretyazhko and G. Sposito, Iron(III) reduction and phosphorous solubilization in humid tropical forest soils, *Geochim. Cosmochim. Acta*, 2005, **69**, 3643–3652, DOI: 10.1016/j.gca.2005.03.045.

3 K. Yu and W. H. Patrick, Redox Range with Minimum Nitrous Oxide and Methane Production in a Rice Soil under Different pH, *Soil Sci. Soc. Am. J.*, 2003, **67**, 1952–1958, DOI: 10.2136/sssaj2003.1952.

4 P. Dalkmann, T. F. Dresemann, C. Siebe, T. Mansfeldt, W. Amelung and J. Siemens, Release of pharmaceuticals under reducing conditions in a wastewater-irrigated mexican soil, *J. Environ. Qual.*, 2014, **43**, 1926–1932.

5 S. Schuth, J. Hurraß, C. Münker and T. Mansfeldt, Redox-dependent fractionation of iron isotopes in suspensions of a groundwater-influenced soil, *Chem. Geol.*, 2015, **392**, 74–86, DOI: 10.1016/j.chemgeo.2014.11.007.

6 K. Dorau, S. Wessel-Bothe, G. Milbert, H. P. Schrey, D. Elhaus and T. Mansfeldt, Climate change and redoximorphosis in a soil with stagnic properties, *CATENA*, 2020, **190**, 104528, DOI: 10.1016/j.catena.2020.104528.

7 T. Mansfeldt, in *Field Measurement Methods in Soil Science*, ed. S. Wessel-Bothe and L. Weihermüller, Borntraeger Science Publishers, Stuttgart, Germany, 2020, pp. 19–41.

8 S. Fiedler and W. R. Fischer, Automatische Meßanlage zur Erfassung kontinuierlicher Langzeitmessungen von Redoxpotentialen in Böden, *J. Plant Nutr. Soil Sci.*, 1994, **157**, 305–308, DOI: 10.1002/jpln.19941570410.

9 J.-Y. Loyer and J. Susini, Réalisation et utilisation d'un ensemble automatique pour la mesure en continu et "in situ" du pH, du Eh et du pNa du sol, *Cahiers ORSTOM.Série Pédologie*, 1978, **16**, 425–437.

10 M. Vorenhout, H. G. van der Geest, D. van Marum, K. Wattel and H. J. P. Eijsackers, Automated and Continuous Redox Potential Measurements in Soil, *J. Environ. Qual.*, 2004, **33**, 1562–1567, DOI: 10.2134/jeq2004.1562.

11 C. Shoemaker, R. Kröger and S. C. Pierce, *Presented in Part at the Mississippi Water Resources Conference*, Jackson, MS, USA, 2012.

12 E. van Bochove, S. Beauchemin and G. Thériault, Continuous Multiple Measurement of Soil Redox Potential Using Platinum Microelectrodes, *Soil Sci. Soc. Am. J.*, 2002, **66**, 1813–1820, DOI: 10.2136/sssaj2002.1813.

13 M. Vorenhout, H. G. van der Geest and E. R. Hunting, An improved datalogger and novel probes for continuous redox measurements in wetlands, *Int. J. Environ. Anal. Chem.*, 2011, **91**, 801–810, DOI: 10.1080/03067319.2010.535123.

14 T. Wanzek, M. Keiluweit, T. Varga, A. Lindsley, P. Nico, S. Fendorf and M. Kleber, The ability of soil pore network metrics to predict redox dynamics is scale dependent, *Soil Syst.*, 2018, **2**, 1–25, DOI: 10.3390/soilsystems2040066.

15 E. R. Hunting, R. G. Harrison, A. Bruder, P. M. van Bodegom, H. G. van der Geest, A. A. Kampfraath, M. Vorenhout, W. Admiraal, C. Cusell and M. O. Gessner, Atmospheric Electricity Influencing Biogeochemical Processes in Soils and Sediments, *Front. Physiol.*, 2019, **10**, 1–10, DOI: 10.3389/fphys.2019.00378.

16 O. N. Forde, A. G. Cahill, R. D. Beckie and K. U. Mayer, Barometric-pumping controls fugitive gas emissions from a vadose zone natural gas release, *Sci. Rep.*, 2019, **9**, 14080, DOI: 10.1038/s41598-019-50426-3.

17 K. Dorau and T. Mansfeldt, Comparison of redox potential dynamics in a diked marsh soil: 1990 to 1993 *versus* 2011 to 2014, *J. Plant Nutr. Soil Sci.*, 2016, **179**, 641–651, DOI: 10.1002/jpln.201600060.

18 L. J. McKenzie, E. P. Whiteside and A. E. Erickson, Oxidation-reduction studies on the mechanism of B horizon formation in Podzols, *Soil Sci. Soc. Am. J.*, 1960, **24**, 300–305, DOI: 10.2136/sssaj1960.03615995002400040026x.

19 J. Glinski and W. Stepniewski, *Soil Aeration and its Role for Plants*, CRC Press, Boca Raton, FL, USA, 1985.

20 T. Borch, R. Kretzschmar, A. Kappler, P. V. Cappellen, M. Ginder-Vogel, A. Voegelin and K. Campbell, Biogeochemical Redox Processes and their Impact on Contaminant Dynamics, *Environ. Sci. Technol.*, 2010, **44**, 15–23, DOI: 10.1021/es9026248.

21 K. W. Yu, Z. P. Wang, A. Vermoesen, W. H. Patrick and O. Van Cleemput, Nitrous oxide and methane emissions from different soil suspensions: effect of soil redox status, *Biol. Fertil. Soils*, 2001, **34**, 25–30, DOI: 10.1007/s003740100350.

22 H. L. Bohn, Redox potentials, *Soil Sci.*, 1971, **112**, 39–45.

23 M. Whitfield, Thermodynamic limitations on the use of the platinum electrode in E_H measurements, *Limnol. Oceanogr.*, 1974, **19**, 857–865, DOI: 10.4319/lo.1974.19.5.0857.

24 T. J. Grundl, S. Haderlein, J. T. Nurmi and P. G. Tratnyek, in *Aquatic Redox Chemistry*, American Chemical Society, 2011, vol. 1071, ch. 1, pp. 1–14.

25 S. C. Mueller, L. H. Stolzy and G. W. Fick, Constructing and screening platinum microelectrodes for measuring soil redox potential, *Soil Sci.*, 1985, **139**, 558–560.

26 H. L. Bohn, B. L. McNeal and G. A. O'Connor, *Soil Chemistry*, John Wiley & Sons, New York, NY, USA, 3rd edn, 2001.

27 R Core Team, 2020.

28 DIN ISO 10390:2005-12, Soil Quality – Determination of pH (ISO 10390:2005), 2005.

29 ISO 10694:1995, *Soil Quality – Determination of Organic and Total Carbon after Dry Combustion (Elementary Analysis)*, 1995.

30 ISO 11277:2020, *Soil Quality – Determination of Particle Size Distribution in Mineral Soil Material — Method by Sieving and Sedimentation*, 2020.

31 D. K. Nordstrom, Thermochemical redox equilibria of ZoBell's solution, *Geochim. Cosmochim. Acta*, 1977, **41**, 1835–1841, DOI: 10.1016/0016-7037(77)90215-0.

32 T. B. Parkin and T. C. Kaspar, Temperature Controls on Diurnal Carbon Dioxide Flux, *Soil Sci. Soc. Am. J.*, 2003, **67**, 1763–1772, DOI: 10.2136/sssaj2003.1763.

33 D. L. Parkhurst and C. A. J. Appelo, User's guide to PHREEQC (Version 2): a computer program for speciation, batch-reaction, one-dimensional transport, and inverse geochemical calculations, *Report 99–4259*, 1999.

34 D. Jacques, J. Šimnek, D. Mallants and M. T. van Genuchten, in *Developments in Water Science*, ed. S. M. Hassanizadeh, R.

This journal is © The Royal Society of Chemistry 2021

Environ. Sci.: Processes Impacts, 2021, **23**, 1782–1790 | **1789**

J. Schotting, W. G. Gray and G. F. Pinder, Elsevier, 2002, vol. 47, pp. 555–562.

35 M. Maisch, U. Lueder, A. Kappler and C. Schmidt, Iron Lung: How Rice Roots Induce Iron Redox Changes in the Rhizosphere and Create Niches for Microaerophilic Fe(II)-Oxidizing Bacteria, *Environ. Sci. Technol. Lett.*, 2019, **6**, 600–605, DOI: 10.1021/acs.estlett.9b00403.

36 IUSS Working Group WRB, *World Reference Base for Soil Resources 2014, Update 2015*, FAO, Rome, Italy, 2015.

37 H. Weigand, T. Mansfeldt, R. Bäumler, D. Schneckenburger, S. Wessel-Bothe and C. Marb, Arsenic release and speciation in a degraded fen as affected by soil redox potential at varied moisture regime, *Geoderma*, 2010, **159**, 371–378, DOI: 10.1016/j.geoderma.2010.08.014.

38 W. J. Catallo, *Hourly and Daily Variation of Sediment Redox Potential in Tidal Wetland Sediments*, U.S. Geological Survey Report USGS/BRD/BSR-1999-0001, Lafayette, LA, 1999.

39 C. A. Seybold, W. Mersie, J. Huang and C. McNamee, Soil redox, pH, temperature, and water-table patterns of a freshwater tidal wetland, *Wetlands*, 2002, **22**, 149–158, DOI: 10.1672/0277-5212.

40 J. Dušek, T. Picek and H. Čížková, Redox potential dynamics in a horizontal subsurface flow constructed wetland for wastewater treatment: Diel, seasonal and spatial fluctuations, *Ecol. Eng*, 2008, **34**, 223–232, DOI: 10.1016/j.ecoleng.2008.08.008.

41 C. D. Wallace, A. H. Sawyer and R. T. Barnes, Spectral analysis of continuous redox data reveals geochemical dynamics near the stream–aquifer interface, *Hydrol. Processes*, 2019, **33**, 405–413, DOI: 10.1002/hyp.13335.

42 D. G. Strawn, H. L. Bohn and G. A. O'Connor, *Soil Chemistry*, John Wiley & Sons, Ltd., Hoboken, NJ, USA, 4th edn, 2015.

43 E. Hering, R. Martin and M. Stohrer, *Taschenbuch der Mathematik und Physik*, Springer Vieweg, Heidelberg, Germany, 2017.

44 H. Galster, *pH Measurement: Fundamentals, Methods, Applications, Instrumentation*, VCH, Weinheim, Germany, 1991.

1790 | *Environ. Sci.: Processes Impacts*, 2021, **23**, 1782–1790

This journal is © The Royal Society of Chemistry 2021